Available online at www.sciencedirect.com
SCIENCE DIRECT
Journal of Catalysis 242 (2006) 82–91
JOURNAL OF CATALYSIS
www.elsevier.com/locate/jcat

Catalytic properties of the novel mesoporous aluminosilicate AlTUD-1

R. Anand [a,b,*], R. Maheswari [b,c], U. Hanefeld [a,*]

[a] *Gebouw voor Scheikunde, Technische Universiteit Delft, Julianalaan 136, 2628 BL Delft, The Netherlands*
[b] *Advanced Chemical Technology Division, Korea Research Institute of Chemical Technology (KRICT), P.O. Box 107, Yusung, Daejeon 305-600, Republic of Korea*
[c] *Institut für Technische Chemie, Universität Stuttgart, Pfaffenwaldring 55, D-70569 Stuttgart, Germany*

Received 26 October 2005; revised 18 May 2006; accepted 20 May 2006

Available online 3 July 2006

Abstract

The novel mesoporous three-dimensional amorphous aluminosilicate, an excellent catalyst carrier denoted as AlTUD-1, was prepared with different Si/Al ratios using a surfactant-free one-pot synthesis with triethanolamine as the template. Characterization of this material by means of XRD and N_2 sorption showed that it is mesoporous with a specific surface area as high as 925 m^2/g. The mesoporosity was further supported by HR-TEM results. ^{27}Al-MAS-NMR spectra of the calcined AlTUD-1 samples proved that almost 60% of Al was tetrahedrally coordinated. NH_3-TPD of AlTUD-1 samples revealed that the number of acid sites decreased and the strength of acid sites increased with increasing Si/Al ratio. The acid sites observed were mainly Lewis acid sites, and the Brønsted acidity generated from Al in tetrahedral coordination was observed to be weak. This novel material with a relatively low aluminum content was shown to be a versatile catalyst for the alkylation of phenol in the gas phase as well as in the liquid phase with *tert*-butyl alcohol and methyl *tert*-butylether, respectively. This demonstrates that a variation in Si/Al ratio can convert a catalyst carrier into a catalyst itself.

Keywords: AlTUD-1; Mesoporous aluminosilicate; Acidity; Friedel–Crafts alkylation; Isomerization; Disproportionation

1. Introduction

For more than a decade, mesoporous molecular sieves (MMSs) have proven valuable. Starting with MCM-41 in 1992 [1,2], various MMSs have been developed, including MCM-48, SBA, and HMS. Aluminum was incorporated into these materials, and their catalytic performance was studied in various acid-catalyzed reactions [3–8]. Due to their large pore diameter of 2–50 nm, they enable the transformation of bulky substrates with large carbon skeletons, a typical feature in fine chemicals. TUD-1, a three-dimensional amorphous mesoporous silica, was first described in 2000 [9,10]. Its straightforward preparation has opened many possibilities for modifying this material, such as the introduction of heteroatoms into its framework [11–14]. The surfactant-free synthesis of TUD-1 makes it environmentally friendly. Its three-dimensional network with a tunable pore size improves substrate accessibility; indeed, virtually no mass transfer limitations are observed compared with other mesoporous materials, such as the one-dimensional MCM-41. Recently, aluminum was introduced into the framework of TUD-1, and the three-dimensional mesoporous aluminosilicate AlTUD-1 was obtained. It is an excellent ionic carrier material for homogeneous transition metal catalysts, several of which were immobilized [15–18]. The Si:Al ratio used in these studies was low (4:1); consequently, the material was only weakly acidic. When the Si:Al ratio is changed the material should become strongly acidic, transforming AlTUD-1 from a carrier material into a catalyst in its own right. Here we describe the synthesis and catalytic properties of this novel mesoporous heterogeneous acid for the preparation of *tert*-butyl phenols.

In general, *tert*-butyl phenols are obtained by alkylation of phenol with different reagents, such as isobutene, *tert*-butyl alcohol (TBA), methyl-*tert*-butyl ether (MTBE), and *tert*-butyl halides. The reaction is carried out in either liquid or vapor phase in the presence of a strongly acidic catalyst, such as sulfuric or phosphoric acids, boron trifluoride, Al-salts, metal oxides, silica gel, silica–alumina, activated clays, ionic liquids, zeolites, mesoporous materials, molecular sieves, or strongly

* Corresponding authors.
E-mail address: u.hanefeld@tudelft.nl (U. Hanefeld).

0021-9517/$ – see front matter
doi:10.1016/j.jcat.2006.05.022

acidic ion-exchange resins, each of which has its own merits and shortcomings [19–31]. For example, using homogeneous catalysts has drawbacks due to their hazardous, corrosive nature and laborious workup. Cationic exchange resins cannot be used at higher temperatures, because they are unstable; moreover, they have low activity and selectivity [21,23]. When using TBA as an alkylation reagent, its in situ dehydration leads to the formation of water as a byproduct in the alkylation reaction. Even though water is a green solvent, it alters the catalyst activity, especially of zeolites. MTBE is a good alternative for the in situ generation of pure isobutylene. The byproduct methanol can be recovered and reused and does not deactivate the solid acids as quickly as water does [30]. The alkylation of phenol in the liquid and gas phases is an interesting test reaction for a solid acidic catalyst, because the main alkylation reaction is in equilibrium with isomerization, disproportionation, and dealkylation reactions of the initial products formed. Varying the reaction conditions should enable the shifting of these equilibria and thus of the product distribution. This allows the investigation of many different parameters of both the reaction and the novel catalyst.

In this work, we report the synthesis of the mesoporous aluminosilicate AlTUD-1 with a wider range of Si:Al ratios (10–100) using triethanolamine (TEA) as a template. The catalytic activity of AlTUD-1 was explored in the liquid-phase alkylation of phenol with MTBE and vapor-phase alkylation of phenol with TBA.

2. Experimental

2.1. Synthesis of AlTUD-1

AlTUD-1 was synthesized using TEA as a template in a one-pot surfactant-free procedure based on the sol–gel technique. AlTUD-1 with varying Si:Al ratios can be synthesized by adjusting the molar ratio of SiO_2:x Al_2O_3:(0.3–0.5) tetraethylammonium hydroxide (TEAOH):(0.5–1) TEA:(10–20) H_2O. In a typical synthesis (Si/Al = 25), 0.68 g of aluminum(III) isopropoxide (98%, Aldrich) dissolved in a 1:1 mixture of isopropanol and ethanol was added to 17.3 g of tetraethyl orthosilicate (98%, Aldrich). After stirring for a few minutes, a mixture of 12.5 g of TEA (97%, ACROS) and 9.4 g of water was added, followed by addition of 10.2 g of tetraethyl ammonium hydroxide (35 wt%, Aldrich) under vigorous stirring. The clear gel obtained after these steps was then aged at room temperature for 12–24 h and dried at 98 °C for 12–24 h, followed by hydrothermal treatment in a Teflon-lined autoclave at 180 °C for 4–24 h and final calcination in the presence of air up to 600 °C at a temperature ramp of 1 °C/min. AlTUD-1 with Si/Al ratios of 10, 25, 50, 75, and 100 were prepared and are denoted as Al-10, Al-25, Al-50, Al-75, and Al-100, respectively.

2.2. Characterization of AlTUD-1

Chemical analyses of Si and Al were performed by dissolving the AlTUD-1 in 1% HF and 1.3% H_2SO_4 solution and measuring them with inductively coupled plasma–optical emission spectroscopy (ICP-OES) on a PerkinElmer Optima 3000DV instrument. Powder X-ray diffraction (XRD) patterns were obtained on a Philips PW 1840 diffractometer equipped with a graphite monochromator using Cu$K\alpha$ radiation (λ = 0.1541 nm). The samples were scanned over a range of 0.1°–80° 2θ with steps of 0.02°. The textural parameters were evaluated from volumetric nitrogen physisorption at 77 K. Before the physisorption experiment, the samples were dried in vacuum at 300 °C, and the nitrogen adsorption and desorption isotherm was measured on the Quantachrome Autosorb-6B at 77 K. The pore size distribution was calculated from the adsorption branch using the Barret–Joyner–Halenda (BJH) model [32]. The BET method was used to calculate the surface area (S_{BET}) of the samples, and the mesopore volume (V_{meso}) was determined by the t-plot method of Lippens and de Boer [33]. Transmission electron microscopy (TEM) was performed using a Philips CM30T electron microscope with a LaB6 filament as the electron source operated at 300 kV.

Temperature-programmed desorption of ammonia measurements were carried out on a Micromeritics TPR/TPD 2900 instrument equipped with a thermal conductivity detector (TCD). The 30-mg sample was pretreated at 550 °C in a flow of He (30 ml/min) for 1 h. Then pure NH_3 (40 ml/min) was adsorbed at 120 °C for 15 min. Subsequently, a flow of He (30 ml/min) was passed through the reactor for 30 min to remove any weakly adsorbed NH_3 from the sample. This procedure was repeated three times. Desorption of NH_3 was monitored in the range of 120–550 °C at a ramp rate of 10 °C/min. The desorption peak was deconvoluted into three peaks at around 200, 300, and 450 °C, corresponding to weak, medium, and strong acid sites using Origin software (version 7.5) by Gaussian fit.

A Nicolet AVATAR 360 FTIR instrument was used to record FTIR spectra. Acid strength distribution was evaluated by IR spectra of adsorbed pyridine. AlTUD-1 samples (15–25 mg/cm^2) wafers were calcined at 500 °C for 2 h under vacuum (10 Pa) in a custom-made vacuum cell with CaF_2 windows. Then the cell was cooled down to room temperature, and the IR spectrum was collected (A). As water and any adsorbed materials were removed by this treatment, hydroxyl spectra were obtained from this sample. Then the temperature of the cell was raised to 100 °C, and the sample was then brought into contact with pyridine vapors (20 Torr) for 30 min. The temperature of the cell was raised to 150 °C, with vacuum applied for 30 min to remove physisorbed and loosely bound pyridine. Subsequently, the temperature of the cell was raised to 200 °C under vacuum for another 30 min. This procedure ensures the removal of all physisorbed pyridine (with only chemisorbed pyridine available for IR analysis). The cell was then cooled to room temperature, and the IR spectra were collected (B). The differential spectra were recorded ((A) and (B)), as shown in Fig. 7. All of the spectra were recorded at room temperature with a resolution of 2 cm^{-1} averaging over 500 scans.

2.3. Catalytic activity of AlTUD-1

The alkylation of phenol with TBA was carried out with a fixed-bed continuous-downflow glass reactor (13 mm i.d.).

About 2 g of AlTUD-1 catalyst of 20–40 mesh size was placed in the reactor and supported on either side with a thin layer of quartz wool and ceramic beads. A mixture of phenol:TBA (1:2) was fed to the catalyst at a weight hourly space velocity (WHSV) of 1 h^{-1} using an infusion syringe pump. The reaction temperatures ranged from 150 to 250 °C.

The liquid-phase alkylation of phenol with MTBE was carried out in a 100-ml batch reactor, a mechanically stirred Parr autoclave (series 4560, Hastalloy C), equipped with a pressure gauge (range 0–40 bar). In a typical reaction, the autoclave was charged with 2 g of a mixture of phenol and MTBE in a molar ratio of 1:2 with 20 ml of cyclohexane (solvent). Then AlTUD-1 (0.2 g), pretreated at 180 °C for 2 h, was added. The autoclave was sealed and heated to the required reaction temperature.

2.4. Analysis

After the gas-phase reaction, the liquid products were collected in an ice-cold condenser. The liquid products were withdrawn from the autoclave. Both types of samples were analyzed on an Agilent 6890 gas chromatograph equipped with a Sil 5 CB capillary column (50 m × 0.53 mm) and a flame ionization detector. The products were identified by the retention time of authentic samples as well as by GC-MS. GC temperature program: isothermal at 100 °C for 14 min, followed by heating to 250 °C with a rate of 5 °C/min and subsequently to 300 °C with a rate of 10 °C/min, final time 10 min at 300 °C. (Retention time in min: 8.35 phenol; 23.50 2-TBP; 24.08 4-TBP; 29.74 2,6-DTBP; 31.08 2,4-DTBP.)

3. Results and discussion

Powder XRD patterns for calcined AlTUD-1 samples (Fig. 1A) showed a single intensive peak at low angle (0.4°–0.8° 2θ) indicating that AlTUD-1 is a meso-structural material. A decrease in intensity with an increase in the content of Al can be noted. No crystalline or segregated phases of alumina were observed by XRD in any of the samples (Fig. 1B). The elemental analysis (Table 1) proves that the Si/Al ratio of the calcined samples is very close to that used in the synthesis gel. It once again implies the predictability of the synthesis method of TUD-1 as observed with other metal-incorporated TUD-1 materials [11–14].

HR-TEM characterizations of AlTUD-1 samples (Fig. 2) revealed the presence of mesopores in these materials and showed that the walls of all AlTUD-1s are amorphous. Only at a very high Al content (sample Al-10, Fig. 2C) could some crystals of alumina be detected by HR-TEM. But even with this sensitive technique, no crystalline alumina was observed for Al-25 or Al-100 (Figs. 2A and 2B), nor was it observed at a very high aluminum content (Si/Al = 4:1) using tetraethyleneglycol as a template in the earlier study [16].

The textural parameters for all AlTUD-1 samples obtained from N_2 sorption studies showed a type IV isotherm (Fig. 3) with a hysteresis loop exhibiting H3-type behavior. The presence of mesopores was evident from the uptake of nitrogen at relative pressures of 0.4–0.8 P/P_0 as a result of nitrogen condensation inside the mesopores. The adsorption of the nitrogen was not linked to a specific pressure, but occurred over a wider range, indicating a rather broad pore size distribution. The difference between the adsorption and desorption proves the presence of percolation or network effects in the pores. Desorption occurs close to the critical pressure of nitrogen (±0.43 P/P_0). Below this critical pressure, the hysteresis will close and adsorption and desorption isotherms should overlay. This closing of the isotherm causes an artefact, called TSE, that appears in the desorption pore size distribution as a narrow distribution of apparent pores [34]. However, the pore size distribution was still significantly narrower than that when tetraethyleneglycol was used as a template [16]. All of the samples except Al-10 showed a surface area as high as 925 ± 25 m^2/g with a pore volume of 0.9 cm^3/g, indicating an incorporation of Al into the framework of TUD-1 (Table 1). The low surface area

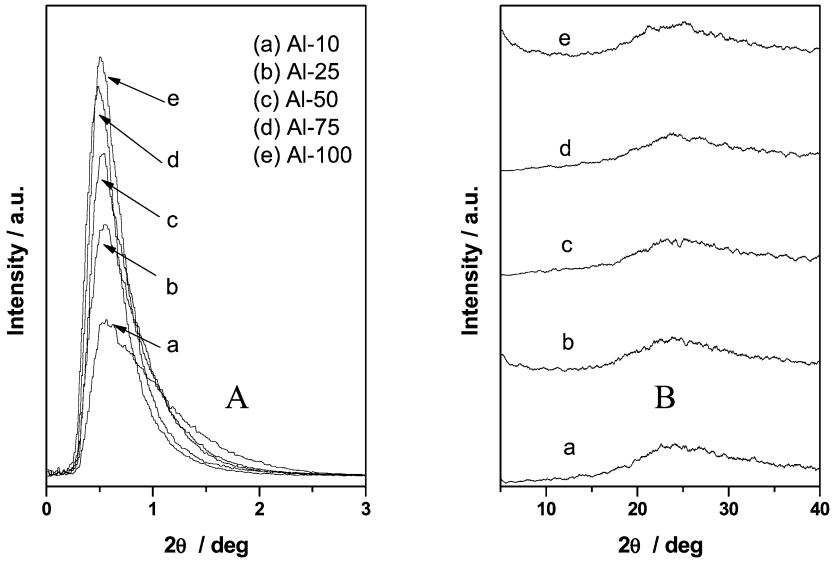

Fig. 1. Powder XRD pattern of calcined AlTUD-1.

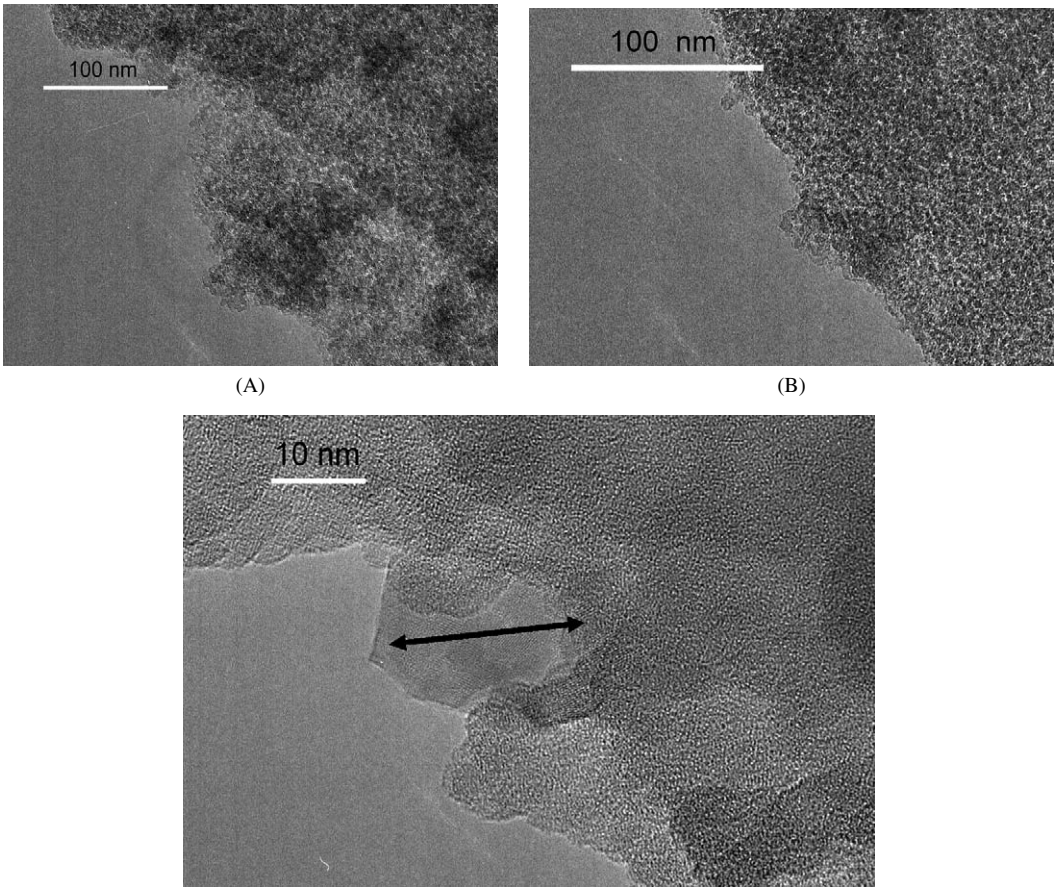

Fig. 2. HR-TEM images of AlTUD-1 Al-100 (A), Al-25 (B) and Al-10 (C).

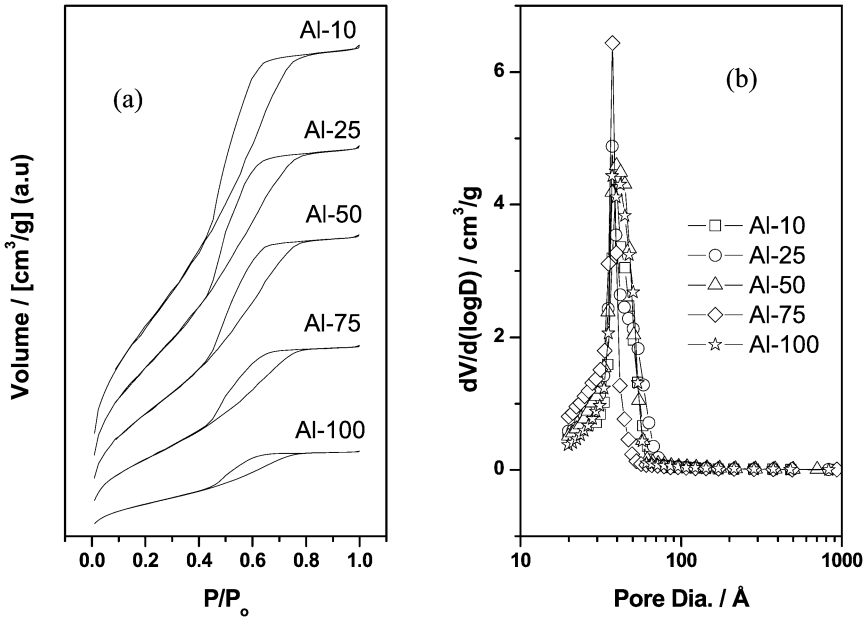

Fig. 3. (a) N_2 sorption isotherms of AlTUD-1; (b) pore size distribution calculated from the adsorption branch using the Barret–Joyner–Halenda (BJH) model [32].

(686 m^2/g) and low pore volume (0.6 cm^3/g) of sample Al-10 compared with the other AlTUD-1 samples may be due to presence of crystalline aluminum oxide, as evident from HR-TEM studies. Because of the low surface area compared with other AlTUD-1 samples, and our interest in studying the catalytic properties of AlTUD-1 with higher Si/Al ratios and thus higher acidity than the earlier-described ionic carrier AlTUD-1 (Si/Al = 4 [15]), we did not consider Al-10 for further studies.

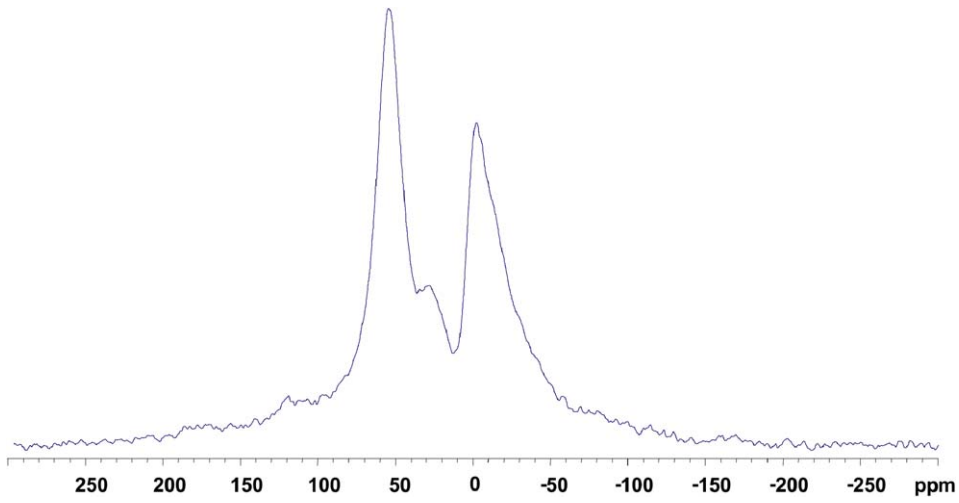

Fig. 4. ^{27}Al MAS NMR spectrum of calcined Al-25 sample.

Table 1
Physico-chemical properties of AlTUD-1

AlTUD-1 (Si/Al)	Si/Al ratio		S_{BET}[b] (m^2/g)	V_{meso}[c] (cm^3/g)	D_{meso}[d] (nm)	mAl/ms[e] (mmol/g)
	Synthesis mixture	After[a] calcination				
Al-10	10	14	686	0.60	3.9	–
Al-25	25	26.6	956	0.95	3.7	1.39
Al-50	50	51.4	970	0.99	3.9	0.72
Al-75	75	78	984	0.88	3.7	0.47
Al-100	100	106	880	0.91	3.7	0.35

[a] From elemental analysis.
[b] Specific surface area.
[c] Specific mesopore volume.
[d] Mesopore diameter.
[e] Al content per weight of solid.

The ^{27}Al MAS NMR spectrum of the calcined sample, Al-25 (Fig. 4), showed the presence of three distinct signals centered around 0, 28, and 55 ppm. The high-field signal corresponds to octahedral aluminum, and that at 55 ppm is assigned to tetrahedral (structural) aluminum. The signal at 27 ppm can be assigned to pentacoordinated aluminum or, alternatively, aluminum in highly distorted tetrahedral sites as found in dealuminated zeolites [35]. Even though a high calcination temperature (600 °C) was applied, only around 40% of Al was present as either octahedral or pentacoordinated species as shown in the ^{27}Al-MAS-NMR spectrum. This spectrum is very similar to that described earlier for AlTUD-1, with tetraethylene glycol used as a template [16].

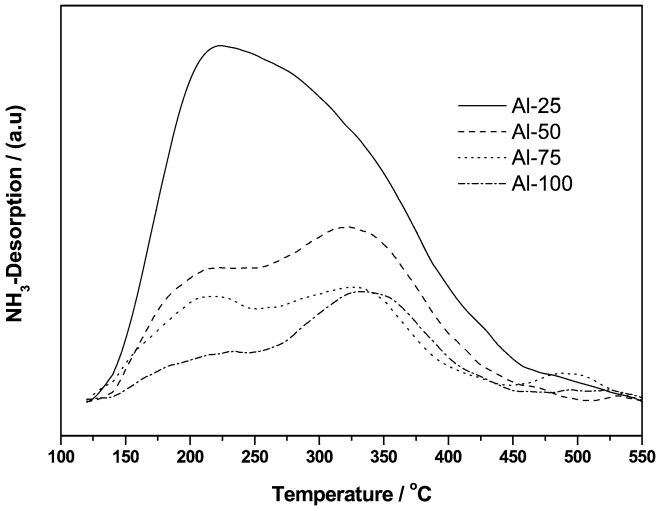

Fig. 5. NH_3-TPD profile for AlTUD-1 with different Si/Al ratios.

The acid site concentration of AlTUD-1 samples was determined by NH_3-TPD (Fig. 5). All of the samples showed a single broad peak of ammonia desorption, suggesting that various types of acid sites with different acid strengths were present. The desorption peak can be deconvoluted into three peaks around at 200, 300, and 450 °C, corresponding to weak, medium, and strong acid sites. The acidity corresponding to these temperatures and the total acidity of these samples are listed in Table 2. It is evident that an increase in the number of acid sites occurred with a decrease in Si/Al ratio. All these

Table 2
Acidic properties of AlTUD-1 from NH_3-TPD

AlTUD-1	T (°C) (center of deconvoluted peak)			mmol NH_3/g			
	Weak	Medium	Strong	Weak[a]	Medium[a]	Strong[a]	Total acidity
Al-25	205	276	365	0.09	0.20	0.08	0.37
Al-50	204	320	465	0.05	0.16	0.01	0.22
Al-75	206	321	489	0.07	0.12	0.02	0.21
Al-100	211	335	505	0.03	0.09	0.01	0.13

[a] Calculated from the area of deconvoluted peak.

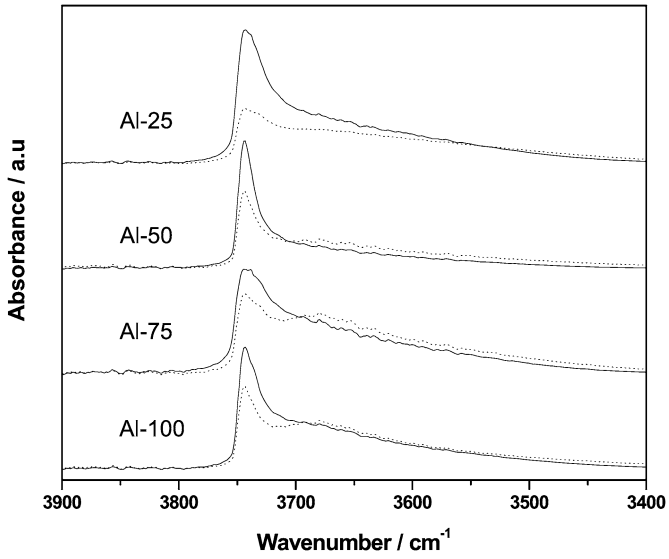

Fig. 6. FTIR spectra of AlTUD-1 samples in the hydroxyl stretching vibration region vacuum treated at 500 °C (—) and after pyridine desorption at 200 °C (···).

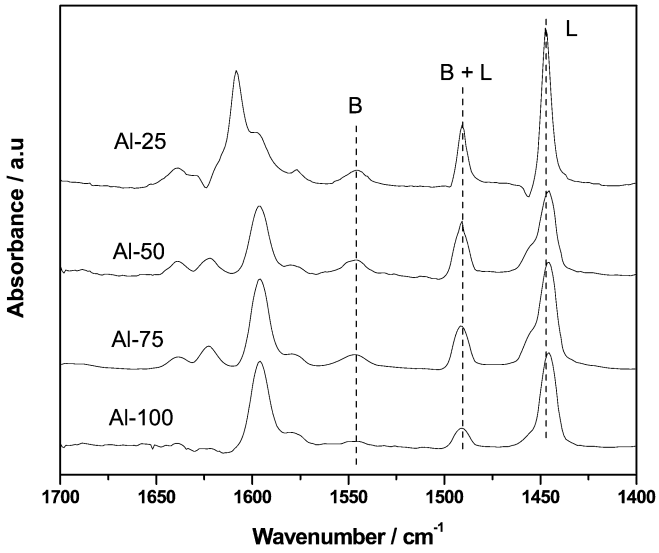

Fig. 7. FTIR difference spectra of AlTUD-1 samples after pyridine desorption at 200 °C.

samples showed a prominent peak around 300–400 °C, demonstrating that the strength of acid sites was of medium acidity. The acid sites at high temperature (>300 °C) are generally considered to be responsible for catalytic activity, and the center of this "medium acid site" peak was shifted to a lower temperature with higher aluminum content, suggesting that, as expected and similar to zeolites, the strength of the acid sites increased with increasing Si/Al ratio. Thus these AlTUD-1 samples have the predicted acidity and should be active as catalysts.

FTIR spectra of AlTUD-1 samples in the hydroxyl stretching vibration region are depicted in Fig. 6. The spectra drawn with a solid line were obtained after calcining the AlTUD-1 samples at 500 °C for 2 h at 10 Pa. The spectra drawn with a dotted line were obtained after pyridine adsorption at 100 °C for 30 min and subsequent desorption at 200 °C for 30 min. All of the spectra showed a peak at 3744 cm^{-1}, corresponding to the terminal silanol groups; the intensity of this peak decreased on adsorption of pyridine. The presence of a broad hump at around 3650 cm^{-1} in all of the spectra after pyridine adsorption and subsequent desorption at 200 °C indicates the interaction of pyridine molecules with the aluminum in the AlTUD-1 samples. Similar observations were also reported for AlSBA-15 [36] and Al-MCM-41 [37].

FTIR spectra of adsorbed pyridine in the 1700–1400 cm^{-1} region for AlTUD-1 samples are depicted in Fig. 7. From the literature [37–39], it is well known that the bands at 1545 and 1455 cm^{-1} are due to pyridine molecules strongly bound to Brønsted acid sites (B) and Lewis acid sites (L), respectively. The band at 1496 cm^{-1} was attributed to pyridine associated with both Lewis and Brønsted acid sites. The concentrations of Brønsted, Lewis, and total acid sites are given in Table 3. An increase in the concentration of Lewis acid sites is clearly visible with an increase in the aluminum content. Similarly, the concentration of Brønsted acid sites increases as well. Overall, the ratio of Lewis acid sites to Brønsted acid sites does not shift significantly. Importantly, the increase in the concentration of Lewis and Brønsted acid sites is much lower than the increase in aluminum content. This again supports the fact that the acidity of AlTUD-1 increases with an increase in the Si/Al ratio. The increase in Lewis acidity corresponds to the observation that for AlSBA-15, the Lewis acidic sites concentration increases with aluminum content. However, unlike AlSBA-15, the acidity of AlTUD-1 is also associated with Brønsted acidity [36].

Table 3
Acidic properties of AlTUD-1 from pyridine adsorption

AlTUD-1	μmol pyridine/g			L/B ratio
	Lewis[a]	Brønsted[a]	Total acidity[a]	
Al-100	7.83	1.46	9.29	5.4
Al-75	8.12	1.88	10	4.3
Al-50	17.34	2.79	20.13	6.2
Al-25	23.64	3.97	27.6	6

[a] Relative concentration.

3.1. Catalytic properties of AlTUD-1

It is well known that in the presence of an acidic catalyst and Lewis and/or Brønsted acid and at high temperatures, MTBE is split into isobutylene and methanol. Similarly, TBA decomposes into isobutylene and water. This isobutylene or its precursor, the carbenium ion, generated in situ can react with phenol, yielding the mono-alkylated products 2-*tert*-butylphenol (2-TBP) and 4-*tert*-butylphenol (4-TBP), which further react with another mole of isobutylene/carbenium ion, yielding di-alkylated products 2,4-di-*tert*-butylphenol (2,4-DTBP) and 2,6-di-*tert*-butylphenol (2,6-DTBP). Scheme 1 illustrates several acid-catalyzed equilibrium reactions that are possible in the *tert*-butylation of phenol with MTBE/TBA. Because AlTUD-1 is an excellent catalyst for the cleavage of ethers, no O-alkylated products were observed.

Fig. 8 shows the results of time on stream for phenol alkylation with TBA in vapor phase over Al-25 at 175 °C and a WHSV of 1 h^{-1}. Phenol conversion increased with time; af-

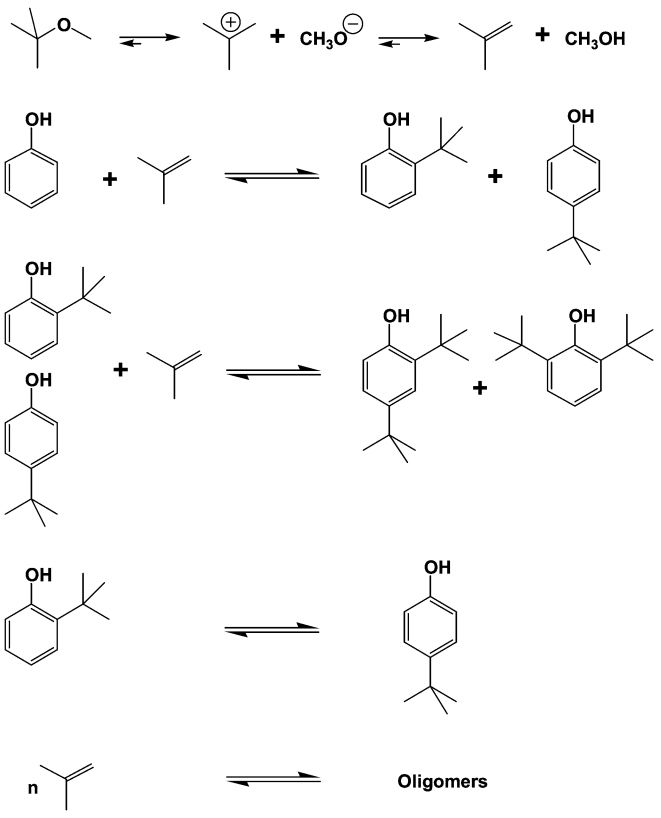

Scheme 1. Several acid-catalyzed equilibrium reactions are possible in the *tert*-butylation of phenol with MTBE/TBA.

ter 2 h, no appreciable change in conversion was noted. This indicates that a steady state was reached in 2 h and that no deactivation of the catalyst occurred during the course of the study. This is attributed to the advantageous random three-dimensional pore system of TUD-1. Several authors observed a decrease in phenol conversion over MCM-41-based catalysts due to the unidimensional pore system of MCM-41 [24,40]. Even for AlSBA-15, a notable decrease in phenol conversion was observed [31]. A moderate increase in 2,4-DTBP formation was observed with a consequent decrease in selectivity for 4-TBP. Because the phenol conversion remained virtually unaltered, this can be explained by secondary reactions of in situ-formed isobutylene with 4-TBP during prolonged reaction runs. In addition, some trialkylation product was formed, and the isobutylene could polymerize. This result confirmed that AlTUD-1 could be an acidic catalyst even at a relatively low Si/Al ratio of 25. Based on these first promising tests of the

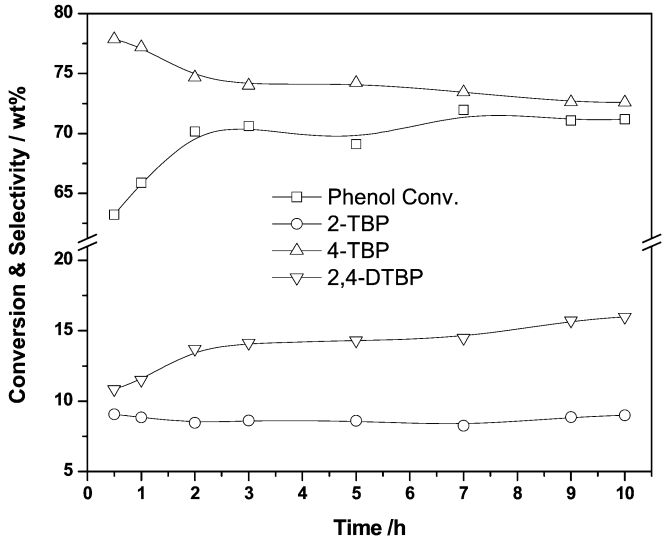

Fig. 8. Time dependence of the gas phase phenol conversion and product selectivity over Al-25 for alkylation of phenol with TBA (ratio 1:2) at 175 °C at a WHSV of 1 h^{-1}.

new material as a catalyst, AlTUD-1s with different Si/Al ratios were included in our study.

The temperature dependence of phenol conversion and product selectivity over AlTUD-1 catalysts with different Si/Al ratios in the alkylation of phenol with TBA at a WHSV of 1 h^{-1} and a TBA/phenol molar ratio of 2 is shown in Fig. 9. Over all AlTUD-1 catalysts, phenol conversion and 2,4-DTBP selectivity decreased with temperature. On the other hand, 4-TBP selectivity increased with temperature, while 2-TBP selectivity remained almost unaltered (6–9%). Only very small differences in phenol conversion and in the selectivity for the products were observed over the different AlTUD-1s. This was expected, because the total acidity increased only modestly with increasing aluminum content. Moreover, the ratio of Lewis acid sites to Brønsted acid sites is very similar (Tables 2 and 3). More importantly, it should be noted that the concentration of aluminum in each reaction decreased. When calculating the conversion of phenol per mmol of aluminum, the true catalytic activity is revealed: The activity increased with increasing Si/Al ratio, in line with the increased acidity per acidic sites (Fig. 9; Tables 1 and 2).

In the liquid-phase alkylation of phenol with MTBE over Al-25 catalyst, an increase in temperature led to an increase in phenol conversion from 33% at 100 °C to 83% at 150 °C (Table 4). A drastic decrease in conversion to 64% was noted with

Table 4
Effect of temperature on the liquid phase alkylation of phenol with MTBE over Al-25[a]

T (°C)	Conversion phenol	Product selectivity						4-TBP/2-TBP
		2-TBP	4-TBP	3-TBP	2,6-DTBP	2,4-DTBP	Others[b]	
100	33.65	50.69	37.19	0.33	0.14	10.03	1.63	0.73
125	55.07	33.84	30.00	0.47	0.45	33.45	1.80	0.89
150	83.15	12.14	43.53	0.10	0.35	40.17	3.72	3.59
175	64.98	9.22	71.89	0.15	0.28	16.77	1.69	7.80

[a] Catalyst: Al-25 (200 mg), time = 4 h, molar ratio phenol/MTBE = 1:2. Reactant: (phenol + MTBE) = 2 g + 20 ml cyclohexane (solvent).
[b] Others include 2,4,6-tri-*tert*-butylphenol and oligomers of isobutene.

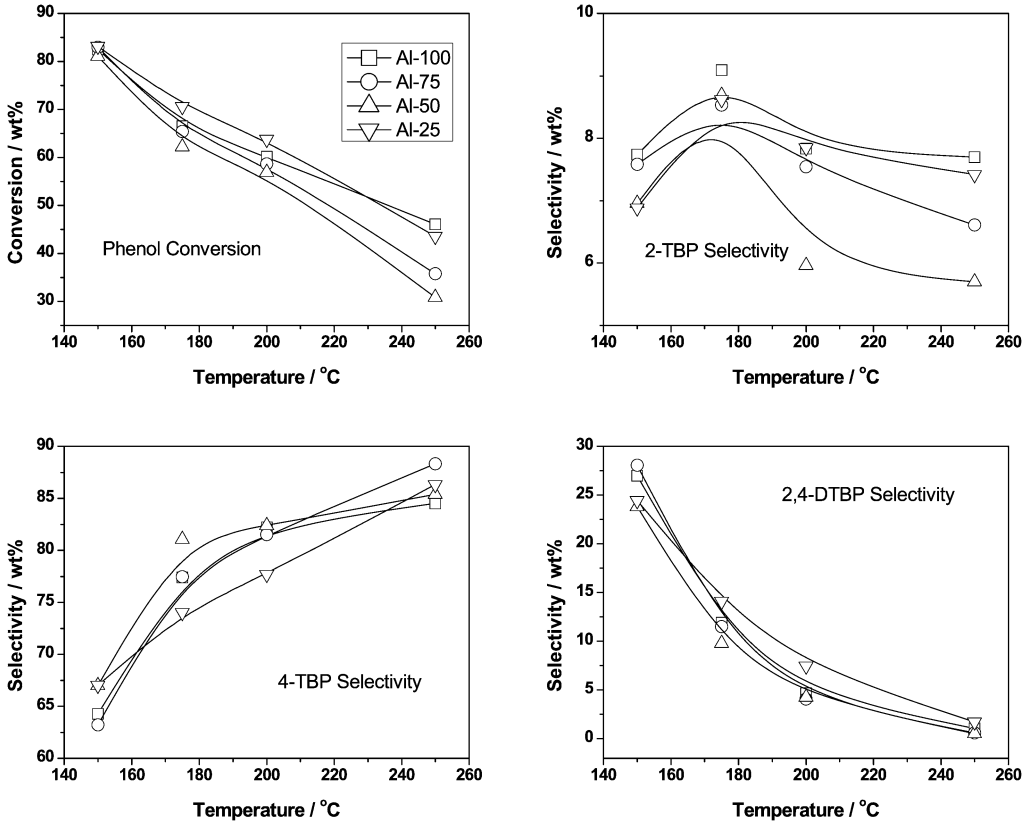

Fig. 9. Temperature dependence of the gas phase phenol conversion and product selectivity over AlTUD-1 with different Si/Al ratios for alkylation of phenol with TBA (ratio 1:2) at a WHSV of 1 h^{-1} for a period of 2 h.

a further temperature increase (to 175 °C). At this high temperature, an increase in 4-TBP was observed as well, attributed to a secondary reaction such as isomerization, disproportionation, dealkylation, and/or transalkylation of 2- or 4-TBP to 2,4-DTBP and phenol, suggesting that the observed Brønsted acid sites were strong enough to carry out these secondary reactions, such as transalkylation, requiring strong acid sites and elevated temperatures [41]. It is also possible that isobutene underwent oligomerization at higher temperatures, which is a competitive reaction to the desired alkylation reaction. At low temperature (100 °C), 2-TBP was formed in excess. It was the kinetically favored product and isomerized to 4-TBP with increasing temperature. The thermodynamically favored product, 3-TBP, and the sterically congested 2,6-DTBP were observed in very low quantities (<0.4%). It is assumed that even if 2,6-DTBP is formed, it readily disproportionates to 2-TBP and phenol or isomerizes to 2,4-DTBP.

To probe this product distribution, reactivity studies of both mono- and di-*tert*-butylphenols (about 2 g in 20 ml of cyclohexane solvent) over Al-25 were carried out; the results (Fig. 10) confirm that these compounds readily underwent isomerization and/or disproportionation/dealkylation to more stable isomers (4-TBP and 2,4-DTBP). Under these reaction conditions, 2-TBP was readily converted (95%) to 4-TBP (65%) and 2,4-DTBP (15%). The isomerization of 4-TBP was slow, as indicated by the very low conversion of 4-TBP (31.32%). A large amount of phenol was produced (44%) with formation of 2,4-DTBP (40%), suggesting that disproportionation/dealkylation was the dominating reaction in this case. Similarly, 2,6-DTBP (99%) was readily isomerized to 2,4-DTBP (44%) and also disproportionated to 4-TBP (44%). The conversion of 2,4-DTBP was significantly lower (45%), yielding mainly the dealkylated product 4-TBP (80%).

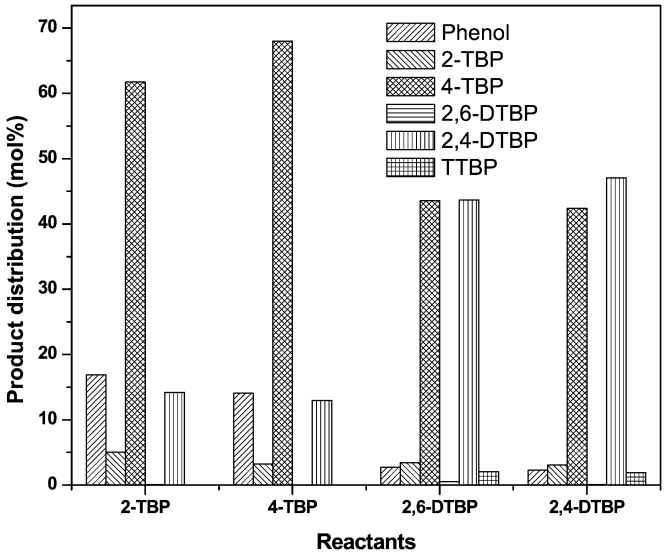

Fig. 10. Product distribution after liquid phase isomerization and disproportionation of mono- and di-*tert*-butylphenols in cyclohexane (solvent) over Al-25 at 150 °C for 2 h. Starting materials are given under the *x* axis.

When varying the phenol to alkylating agent (TBA or MTBE) molar ratio over Al-25, similar trends were observed

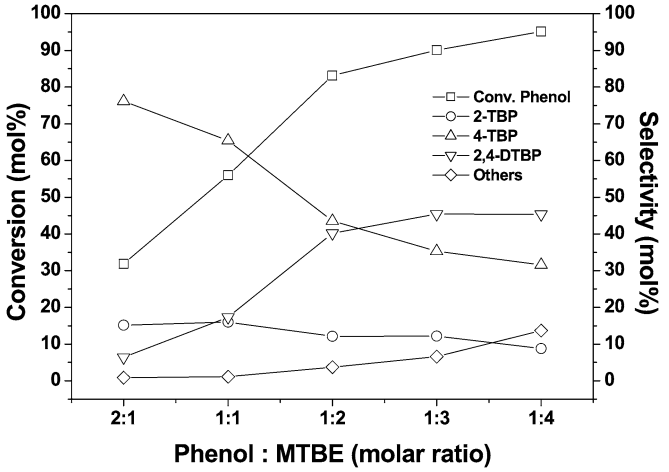

Fig. 11. Effect of phenol:MTBE molar ratio over Al-25 at 150 °C, in liquid phase. Catalyst: AlTUD-1 (Si/Al = 25) (0.200 g, 10 wt% of reactant), $T = 150$ °C, time = 4 h, reactant: (phenol + MTBE) = 2 g + 20 ml cyclohexane (solvent).

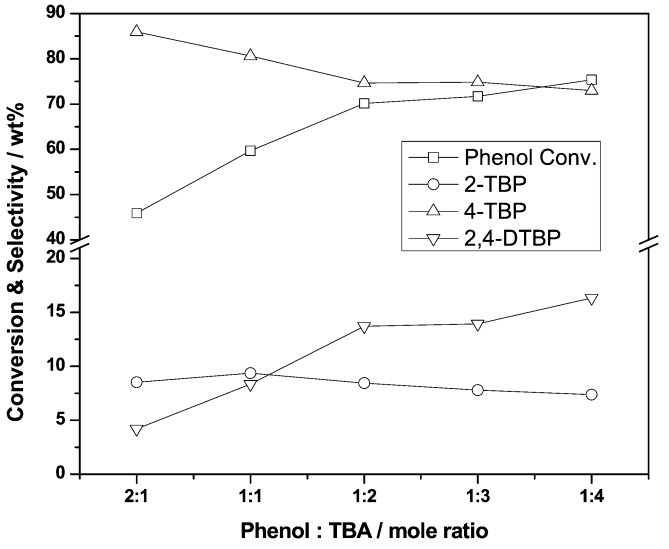

Fig. 12. Effect of phenol:TBA molar ratio over Al-25 at 175 °C, in gas phase at a WHSV of 1 h^{-1} for a period of 2 h.

in the gas and liquid phases (Figs. 11 and 12). A proportional increase in phenol conversion was observed up to a MTBE or TBA/phenol ratio of 2. As expected, a higher selectivity to dialkylation was observed when an excess of alkylating agent was present. A large number of byproducts (oligomers) and polyalkylated phenols, especially 2,4,6-TTBP, were observed with MTBE or TBA/phenol ratios >2. With an increase in phenol/MTBE or TBA ratio, an increase in monoalkylation particularly selective to 4-TBP was observed. The results are in line with observations reported for Al-MCM-41, Al-MCM-48, and Al-SBA-15 catalysts.

Changing the WHSV from 0.5 to 4 h^{-1} induced only very minor differences in phenol conversion and product selectivity (Fig. 13). Al-25 was used as the catalyst at 175 °C with a TBA/phenol molar ratio of 2. This clearly suggests that all of the acid sites were accessible even at a high WHSV of 4 h^{-1}. This demonstrates the advantage of TUD-1 with a random net-

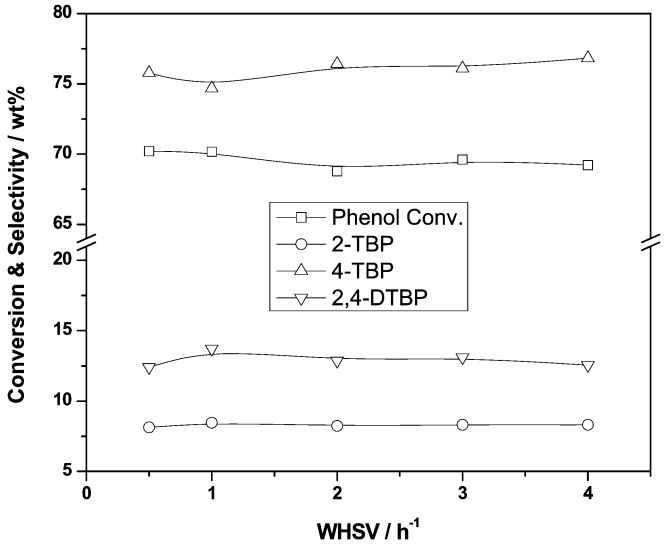

Fig. 13. Effect of WHSV on phenol conversion and product selectivity over Al-25 for the gas phase alkylation of phenol with TBA at 175 °C.

work of pores with a pore size distribution of 4 nm; no diffusion limitation for reactants and products were induced in the range studied.

4. Conclusion

The novel amorphous mesoporous aluminosilicate, AlTUD-1, was prepared with different Si/Al ratios using a surfactant-free one-pot synthesis procedure with triethanolamine as the template. By decreasing the Al content, AlTUD-1 was converted from a weakly acidic, versatile catalyst carrier to a catalyst itself. XRD and HR-TEM images of AlTUD-1 demonstrated that at the catalytically useful Si/Al ratios of 25, 50, 70, and 100, all aluminum was framework-incorporated. Nitrogen sorption studies gave evidence of the mesoporosity of these samples with a relatively narrow pore size distribution around 4 nm, narrower than when tetraethyleneglycol was used as a template [16]. Ammonia TPD measurements showed a broad peak corresponding to the presence of different acid sites with varying strengths. The acidity of the samples followed the extent of Al incorporation. FTIR studies of pyridine adsorption gave evidence of the availability of both Lewis and Brønsted acidity in AlTUD-1. An increase in Al content led to more Lewis and Brønsted acid sites. Thus Al-25, Al-50, Al-75, and Al-100 have the predicted acidity and structure that make them ideal solid acid catalysts.

This was proven in the liquid- and gas-phase alkylation of phenol with MTBE and TBA, respectively. The Brønsted acidity arising from the aluminum incorporation catalyzed the Friedel–Crafts reactions: alkylation of phenol, isomerization, and disproportionation to mono- and di-*tert*-butyl phenols. The selectivity to either monoalkylation or dialkylation can be tuned by varying different parameters. High *para* selectivity can be obtained by using a low alkylating agent-to-phenol ratio in the feed or by increasing the temperature (leading to dealkylation of dialkylated and polyalkylated phenols). These catalysts displayed a stable conversion and product distribution in the gas-

phase reaction for 10 h. As expected for this three-dimensional mesoporous material, no diffusion limitations for reactants or products were observed in the range studied. Consequently, AlTUD-1 is not only an excellent carrier material for catalysts, but also a versatile catalyst in its own right.

Acknowledgments

The authors thank Professor T. Maschmeyer for enabling this research and Dr. Ugo Lafont of DCT/NCHREM, Technische Universiteit Delft, for performing the electron microscopy investigations. U. H. thanks the Royal Netherlands Academy of Arts and Sciences (KNAW) for a fellowship.

References

[1] C.T. Kresge, M.E. Leonowicz, W.J. Roth, J.C. Vartuli, J.S. Beck, Nature 359 (1992) 710.
[2] J.S. Beck, J.C. Vartuli, W.J. Roth, M.E. Leonowicz, C.T. Kresge, K.D. Schmitt, C.T.-W. Chu, D.H. Olson, E.W. Sheppard, S.B. McCullen, J.B. Higgins, J.L. Schlenke, J. Am. Chem. Soc. 114 (1992) 10834.
[3] A. Corma, Chem. Rev. 97 (1997) 2373.
[4] S.K. Jana, H. Takahashi, M. Nakamura, M. Kaneko, R. Nishida, H. Shimizu, T. Kugita, S. Namba, Appl. Catal. A Gen. 245 (2003) 33.
[5] M. Onaka, N. Hashimoto, Y. Kitabata, R. Yamasaki, Appl. Catal. A Gen. 241 (2003) 307.
[6] O. Collart, P. Cool, P. Van der Voort, V. Meynen, E.F. Vansant, K. Houthoofd, P.J. Grobet, O.I. Lebedev, G. Van Tendeloo, J. Phys. Chem. B 108 (2004) 13905.
[7] J.J. Chiu, D.J. Pine, S.T. Bishop, B.F. Chmelka, J. Catal. 221 (2004) 400.
[8] A. Sayari, Chem. Mater. 8 (1996) 1840.
[9] J.C. Jansen, Z. Shan, L. Marchese, W. Zhou, N. van der Puil, Th. Maschmeyer, J. Chem. Soc., Chem. Commun. (2001) 713.
[10] Z. Shan, Th. Maschmeyer, J.C. Jansen, Delft University of Technology, ABB Lummus Global Inc., WO 00/15 551, 2000.
[11] Z. Shan, E. Gianotti, J.C. Jansen, J.A. Peters, L. Marchese, Th. Maschmeyer, Chem. Eur. J. 7 (2001) 1437.
[12] M.S. Hamdy, R. Anand, Th. Maschmeyer, U. Hanefeld, J.C. Jansen, Chem. Eur. J. 12 (2006) 1782.
[13] M.S. Hamdy, G. Mul, J.C. Jansen, A. Ebaid, Z. Shan, A.R. Overweg, Th. Maschmeyer, Catal. Today 100 (2005) 255.
[14] M.S. Hamdy, G. Mul, W. Wei, R. Anand, U. Hanefeld, J.C. Jansen, J.A. Moulijn, Catal. Today 110 (3–4) (2005) 264.
[15] C. Simons, U. Hanefeld, I.W.C.E. Arends, A.J. Minnaard, Th. Maschmeyer, R.A. Sheldon, Chem. Commun. (2004) 2830.
[16] C. Simons, U. Hanefeld, I.W.C.E. Arends, R.A. Sheldon, Th. Maschmeyer, Chem. Eur. J. 10 (2004) 5829.
[17] C. Simons, U. Hanefeld, I.W.C.E. Arends, Th. Maschmeyer, R.A. Sheldon, J. Catal. 239 (2006) 212.
[18] C. Simons, U. Hanefeld, I.W.C.E. Arends, Th. Maschmeyer, R.A. Sheldon, Adv. Synth. Catal. 348 (2006) 471.
[19] V.D. Ryabov, T.S. Golodnaya, Zh. Prikl. Khim. 39 (1966) 2379.
[20] Y. Kamitori, M. Hojo, R. Masuda, T. Izumi, S. Tsukamoto, J. Org. Chem. 49 (1984) 4161.
[21] R.A. Rajadhyaksha, D.D. Chaudhari, Ind. Eng. Chem. Res. 26 (1987) 1276.
[22] B. Chaudhuri, M.M. Sharma, Ind. Eng. Chem. Res. 30 (1991) 227.
[23] K.G. Chandra, M.M. Sharma, Catal. Lett. 19 (1993) 309.
[24] R.F. Parton, J.M. Jacobs, D.R. Huybrechts, P.A. Jacobs, Stud. Surf. Sci. Catal. 46 (1989) 163.
[25] A. Corma, H. Garcia, J. Primo, J. Chem. Res. Synop. 1 (1998) 40.
[26] K. Zhang, H. Zhang, G. Xu, S. Xiang, D. Xu, S. Liu, H. Li, Appl. Catal. 207 (2001) 183.
[27] A. Sakthivel, S.K. Badamali, P. Selvam, Microporous Mesoporous Mater. 39 (2000) 457.
[28] R. Anand, R. Maheswari, K.U. Gore, B.B. Tope, J. Mol. Catal. A Chem. 193 (2003) 251.
[29] P. Selvam, S.E. Dapurkar, Catal. Today 96 (2004) 135.
[30] G.D. Yadav, N.S. Doshi, Appl. Catal. A Gen. 236 (2002) 129.
[31] A. Vinu, B.M. Devassy, S.B. Halligudi, W. Böhlmann, M. Hartmann, Appl. Catal. A Gen. 281 (1–2) (2005) 207.
[32] E.P. Barret, L.G. Joyner, P.H. Halenda, J. Am. Chem. Soc. 73 (1951) 373.
[33] B.C. Lippens, J. de Boer, J. Catal. 4 (1965) 319.
[34] J.C. Groen, L.A.A. Peffer, J. Pérez-Ramírez, Microporous Mesoporous Mater. 60 (2003) 1.
[35] A. Samoson, E. Lippmaa, G. Engelhardt, U. Lohse, H.G. Jerschkewitz, Chem. Phys. Lett. 134 (1987) 589.
[36] Z. Luan, J.A. Fournier, Microporous Mesoporous Mater. 79 (2005) 235.
[37] A. Jentys, N.H. Phan, H. Vinek, J. Chem. Soc. Faraday Trans. 93 (1996) 3287.
[38] J.-H. Kim, M. Tanabe, M. Niwa, Microporous Mater. 10 (1997) 85.
[39] T. Barzetti, E. Selli, D. Moscotti, L. Forni, J. Chem. Soc. Faraday Trans. 92 (1996) 1401.
[40] A. Vinu, K. Usha Nandhini, V. Murugesan, W. Böhlmann, V. Umamaheswari, A. Pöppl, M. Hartmann, Appl. Catal. A Gen. 265 (1) (2004) 1.
[41] M.A. Harmer, Q. Sun, A.J. Vega, W.E. Farneth, A. Heidekum, W.F. Hoelderich, Green Chem. 2 (2000) 7.